Available online at www.sciencedirect.com
ScienceDirect
Catalysis Today 128 (2007) 235–244
CATALYSIS TODAY
www.elsevier.com/locate/cattod

Effect of the redox treatment of Pt/TiO_2 system on its photocatalytic behaviour in the gas phase selective photooxidation of propan-2-ol

M.A. Aramendía [a], J.C. Colmenares [a], A. Marinas [a,*], J.M. Marinas [a], J.M. Moreno [a], J.A. Navío [b], F.J. Urbano [a]

[a] *Organic Chemistry Department, University of Córdoba, Campus de Rabanales, Marie Curie Building, E-14014 Córdoba, Spain*
[b] *Instituto de Ciencia de Materiales de Sevilla, Centro Mixto Universidad de Sevilla-CSIC, Américo Vespucio s/n, E-41092 Sevilla, Spain*

Available online 4 September 2007

Dedicated to Professor Miguel Yus on the occasion of his 60th birthday.

Abstract

Several titania systems were synthesized by the sol–gel method using two different titanium precursors (titanium isopropoxide or tetrachloride) and diverse ageing methods (magnetic stirring, sonication, reflux and microwave radiation). Screening of such different synthetic conditions led us to choose titanium isopropoxide as the titanium precursor and sonication as the method of choice for ageing the gel. Application of the method to the synthesis of a platinum-doped system resulted in a solid with a BET surface area of 57 m^2/g and consisting of 100% anatase titania. The system was submitted to different oxidative and reductive treatments in order to study the effect of such treatments on catalytic performance in gas-phase selective photooxidation of propan-2-ol. Interestingly, both oxidation and reduction at 850 °C led to an increase in molar conversion and selectivity to acetone as compared to calcination at 500 °C. So much so, that oxidation at 850 °C either in synthetic air flow or in static air resulted in better catalytic performance than Degussa P25, despite the fact that our catalysts consisted in very low surface area (6–8 m^2/g) rutile titania specimens. XPS analyses of the systems showed that thermal treatment at 850 °C resulted in electron transfer from titania to Pt^0 particles through the so-called strong metal-support interaction (SMSI) effect. Furthermore, the greater the SMSI effect, the better the catalytic performance. Improvement in photocatalytic activity is explained in terms of avoidance of electron–hole recombination through the electron transfer from titania to platinum particles.

Keywords: Photocatalysis; Selective photooxidation; Titania-based catalysts; Platinum-doped catalyst; Sonication; Microwave treatment; Isopropanol; Sol–gel synthesis; Strong metal-support interaction (SMSI) effect

1. Introduction

Titania is a very versatile material with attractive applications as pigment in paintings, in the production of electrochemistry electrodes, capacitors, solar cells, catalysis and photocatalysis. Regarding the latter application, the possibility of carrying out selective photooxidations in non-aqueous media is very interesting in the context of Green Chemistry [1,2]. TiO_2 is known to exist in three main crystalline forms: brookite, rutile and anatase. Up to now, the best photocatalytic specimens are mainly formed by anatase. Therefore, it seems that potentially active titania particles should possess high surface area and consist exclusively or predominantly in anatase nanoparticles. The most-widely used method to produce titania is the sol–gel one. Such a method requires subsequent calcination of the gel which leads to an increase in crystallite size and a decrease of surface area which could be detrimental to photoactivity. On the other hand, the use of non-conventional irradiation methods (e.g., sonication and microwave radiation) during the synthesis could be of help in order to avoid or diminish crystallite growth.

Moreover, TiO_2 presents a relatively high electron–hole recombination rate which is detrimental to its photoactivity. In this sense, doping with metals such as Pt constitutes an additional method to improve photocatalytic activity of titania since it could make a double effect: (i) firstly, it could shift the

* Corresponding author. Tel.: +34 957218622; fax: +34 957212066.
E-mail address: alberto.marinas@uco.es (A. Marinas).

0920-5861/$ – see front matter © 2007 Elsevier B.V. All rights reserved.
doi:10.1016/j.cattod.2007.07.009

UV–vis absorption to the visible region [3] and (ii) secondly, metals could provoke a decrease in electron–hole recombination rate, acting as electron traps [4].

Furthermore, VIII group metals supported on reducible supports (typically TiO_2) present the so-called strong metal-support interaction (SMSI) effect when reduced at high temperatures as reported originally by Tauster et al. [5]. Over the years after the first discovery of SMSI it has been recognised that hydrogen reduction is not necessary to observe the SMSI effect since it also occurs by vacuum treatment [6] or under oxidizing conditions [7]. A number of models have been proposed to explain this phenomenon, but there are two main proposals: that the effect is due to an electronic perturbation of the metal function (e.g., a charge transfer effect, as first stated by Tauster et al. [5]) or that it is due to encapsulation by some form of TiO_2 [8–10], which acts as a site blocker. In any case, the SMSI effect makes a high temperature treated metal/TiO_2 catalyst behave differently to the low temperature reduced one.

In a previous paper [11], different titania-based systems doped with transition metals (Ag, Fe, Pd, Pt, Zn and Zr) were synthesized by the sol–gel method using titanium tetraisopropoxide as the titanium precursor and both ultrasonic radiation or magnetic stirring as the ageing procedure. Results obtained on that preliminary study prompted us to expand the screening of synthetic conditions in the present piece of research to include another titanium precursor (titanium tetrachloride) and two additional aging procedures (microwave and reflux) and further apply such optimised conditions to the synthesis of a platinum-based system. The resulting catalyst was exposed at high temperature under reducing or oxidizing atmosphere. Catalysts were characterized from textural and structural point of view and tested for the gas-phase photocatalytic selective oxidation of propan-2-ol [12].

2. Experimental

2.1. Synthesis of different titania-based systems

Firstly, 0.25 mmol of the corresponding titanium precursor (76 mL of titanium tetraisopropoxide (TTIP) or 27.48 mL of $TiCl_4$) were added dropwise to a beaker containing 270 mL of a isopropanol:water (10:1, v/v) mixture, under vigorous stirring at 0 °C; pH was then reduced to 2.5 with 60% HNO_3 and sol samples were left under vigorous stirring, at 0 °C for 3 h. Subsequently, pH was increased up to 9 with 5N NH_4OH to form the gel which was divided into four equivalent portions submitted to different ageing methods. The first portion was magnetically stirred for 24 h (ST) and the second one heated under vigorous stirring at propan-2-ol reflux temperature (R). The two final portions were heated for 10 h using non-conventional methods: ultrasonic (US) or microwave (MW) radiation. In the former case, an Ultrasonic Homogenizer (4710 Series, Cole–Palmer Instrument Co. 300 W, 20 kHz, operated in the continuous mode) was used. Moreover, the mixture was kept at 5 °C to avoid solvent evaporation. In the latter case, microwave treatment was performed in a CEM Focused Microwave™ Synthesis system (Model Discover) operating at a continuous microwave power of 140 W. The resulting gels were filtered under vacuum and washed with an aqueous solution of NH_4OH at pH 9. They were then dried at 110 °C for 24 h, ground and sifted to a fine powder (particle diameter below 0.149 mm). Finally, xerogels were calcined at 500 °C for 6 h in static air. Nomenclature of pure titania systems include a letter A or B indicating the precursor used (titanium isopropoxide or titanium tetrachloride, respectively) and a suffix in brackets referring to whether the ageing of the gel was carried out under reflux (R), microwave radiation (MW) ultrasonic irradiation (US) or magnetic stirring (ST).

In the case of platinum-doped system, the acetylacetonate dissolved in 110 mL of isopropanol:water mixture (10:1, v/v) was added dropwise simultaneously to the addition of TTIP, as shown in Fig. 1. For simplification, the platinum-doped titania system was labeled as Pt-AS, the suffix AS standing for ‘‘as synthesized’’ in order to differentiate it of the systems resulting from subsequent thermal treatments. Calcination of Pt-AS in a H_2/Ar (10:90, v/v) flow at 200, 500 or 850 °C for 1 h yielded the systems labeled as Pt-200-H, Pt-500-H and Pt-850-H, respectively. On the other hand, oxidation of Pt-AS either in synthetic air flow or in a furnace in static air at 850 °C for 1 h led to the systems labelled as Pt-850-AIR and Pt-850-F, respectively.

2.2. Characterization

Elemental analysis of Pt-sample was carried out by the staff at the Central Service for the support of research (SCAI) at the University of Córdoba. Measurement was made on a ICP-MS ELAN-DRC-e (Perkin-Elmer), after dissolution of the sample in a H_2SO_4:HF:H_2O (1:1:1) mixture. Atomic spectroscopy standard PE Pure Plus no. 4 (Perkin-Elmer) was used for calibration.

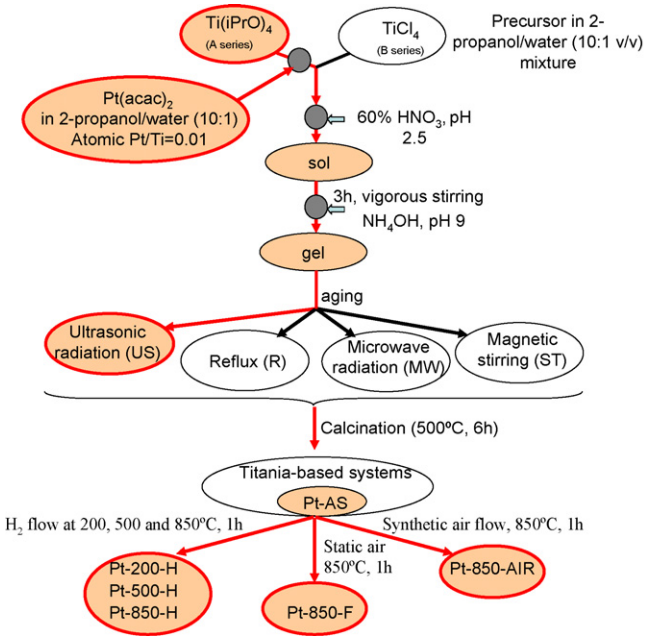

Fig. 1. Schematic representation of synthetic procedure to obtain pure- and platinum-containing titania systems used in the present work.

Thermogravimetric analysis and differential thermal analysis were recorded on a Setaram Setsys 12 instrument. Temperature was ramped from 50 up to 1100 °C at 10 °C min^{-1}. Experiments were carried out in an argon atmosphere (40 mL min^{-1}).

TEM images (carried out at the SCAI of the University of Córdoba) were recorded in a JEOL JEM 2010 microscope operating at an accelerating voltage of 200 kV. The structural resolution of this microscope is 0.19 nm. Samples were previously embedded in an epoxy resin. Sections with a thickness of 40 nm were finally obtained with an ultramicrotome and mounted on 3-mm holey carbon copper grids. Moreover, the microscope was equipped with an EDX detector.

The textural properties of solids (specific surface area, pore volume and mean pore radius) were determined from nitrogen adsorption–desorption isotherms at liquid nitrogen temperature by using a Micromeritics ASAP-2010 instrument. Surface areas were calculated by the BET method, while pore distributions were determined by the BJH method. Prior to measurements, all samples were degassed at 110 °C to 0.1 Pa.

X-ray analysis of solids was carried out using a Siemens D-5000 diffractometer provided with an automatic control and data acquisition system (DACO-MP). The patterns were run with nickel-filtered copper radiation (λ = 1.5406 Å) at 40 kV and 30 mA; the diffraction angle 2θ was scanned at a rate of 2° min^{-1}. The average crystallite size of anatase and rutile was determined according to the Scherrer equation using the full-width at half-maximum (FWHM) of the peak corresponding to 101 and 110 reflections, respectively, and taking into account the instrument broadening.

FT-Raman spectra were obtained on a Perkin-Elmer 2000 NIR FT-Raman system with a diode pumped Nd:YAG laser (9394.69 cm^{-1}). It was operated at a resolution of 4 cm^{-1} throughout the 3600–200 cm^{-1} range to gather 64 scans. Laser power was set at 300 mW.

Diffuse reflectance UV–vis spectra were performed on a Cary 1E (Varian) instrument, using barium sulphate as reference material. Band gap values were obtained from the plot of the modified Kubelka–Munk function $[F(R_\infty)E]^{1/2}$ versus the energy of the absorbed light E. Extrapolation to $y = 0$ of the linear regression in the 3.4–3.7 eV range afforded the band gap energy E_{gap} (eV) [13,14]. Regarding absorption threshold, it was determined according to the formula [15]:

$$\lambda = \frac{hc}{E_{gap}} = \frac{1240}{E_{gap}}$$

TPR analyses were performed on a Micromeritics TPD-TPR 2900 analyzer. Five hundred milligrams of Pt-AS catalyst were placed in the sample holder and reduced in a 45 mL min^{-1} H_2/Ar (10:90) flow. Temperature was ramped between 0 and 850 °C at 10 °C min^{-1}. The final temperature was kept for 1 h and the catalyst was then cooled down to room temperature in an Ar flow (45 mL min^{-1}), thus obtaining the system labelled as Pt-850-H. Once TPR profiles had been registered, new reductive treatments were carried out at intermediate temperatures (200 and 500 °C) which yielded the systems Pt-200-H and Pt-500-H, respectively.

XPS data were recorded on 4 mm × 4 mm pellets, 0.5 mm thick, prepared by slightly pressing the powdered materials which were outgassed in the prechamber of the instrument at 150 °C up to a pressure $\leq 2 \times 10^{-8}$ Torr to remove chemisorbed volatile species (water, CO, etc.) from their surfaces. The Leibold–Heraeus LHS10 spectrometer main chamber, working at a pressure $\leq 2 \times 10^{-9}$ Torr, was equipped with an EA-200 MCD hemispherical electron analyzer with a dual X-ray source working with Al Kα ($h\upsilon$ = 1486.6 eV) at 120 W, 30 mA using C(1s) as energy reference (284.6 eV).

2.3. Photocatalytic reaction

In photocatalytic experiments, 20 mL min^{-1} of a He:O_2 (90:10, v/v) mixture previously bubbled through propan-2-ol at 0 °C was allowed into the photocatalytic reactor (propan-2-ol gas flow was measured to be ca. 8 μmol min^{-1}), in which 30 mg of catalyst had been placed. The fix bed of the catalyst is in contact with the gas flow. UV light (UV Spotlight source Lightningcure™ L8022, Hamamatsu, maximum emission at 365 nm) was focalized on the sample compartment through an optic fiber. Radiant flux in the catalyst compartment was measured to be 1.1 W cm^{-2} (Hamamatsu UV-meter, C6080-03 Model). Reactor was on-line connected to a HP6890 chromatograph equipped with a six-way valve, a HP-PLOTU column (30 m long, 0.53 mm ID, 20 μm film thickness) and a Ni methanator (Agilent Part Number G2747A) which allowed us to determine the percentage of CO_2 resulting from mineralization of propan-2-ol. Further details on the photocatalytic device are given elsewhere [11].

3. Results and discussion

3.1. Pure titania systems

3.1.1. Catalyst characterization

Thermal study of the precursors was carried out and TGA profiles obtained for pure-titania systems (not represented) showed that in all cases the loss of weight is in the range 19.8–22.1%. As for the DTA profiles, all systems exhibit an endothermal peak centered at around 115 °C and most of them (the exception are TiO_2B-MW and TiO_2B-R systems) an exothermal peak in the range 356–447 °C. The former is due to the loss of water adsorbed at the surface of the solid, whereas the latter can be attributed to amorphous to anatase transformation, referred to as glow exotherm [16]. Despite the relatively wide-range of crystallisation temperatures (356–447 °C), no dependence on the titanium precursor or ageing method is observed. In any case, crystallization seems to have been completed at 500 °C which prompted us to choose such a value as calcination temperature.

Textural properties of the solids are summarized in Table 1, including the BET surface area, cumulative pore volume and pore diameter. All systems exhibited type IV isotherms, associated to mesoporous solids, according to Brunauer, Deming, Deming and Teller (BDDT) classification [17]. Hysteresis loops are H1 or H3 types (De Boer classification)

Table 1
Characterization of the different titania-based solids: thermal study of the precursor, compositional and textural analysis

Catalyst	UV–vis		XRD		N_2 isotherms[a]		
	Band gap (eV)	Absorption threshold (nm)	Crystal phases[b] (%)	Crystallite size of anatase (nm)	S_{BET} (m^2/g)	V_p (mL/g)	d_p (Å)
TiO_2A-ST	3.19	389	A/R (97:3)	28	35	0.16	162
TiO2A-R	3.19	389	A (100)	19	60	0.24	142
TiO2A-MW	3.19	389	A (100)	17	71	0.28	129
TiO_2A-US	3.19	389	A (100)	20	121	0.29	93
TiO_2B-ST	2.98	416	A (100)	18	70	0.20	92
TiO2B-R	2.99	415	A/B (96:4)	17	83	0.22	87
TiO2B-MW	3.09	401	A/B (98:2)	15	75	0.15	63
TiO_2B-US	2.98	416	A (100)	24	53	0.12	78

[a] Specific surface area (S_{BET}), cumulative pore volume (V_p) and pore mean diameter (d_p).
[b] Anatase (A), rutile (R) or brookite (B).

[18] for B or A series, respectively. Ageing method seems to affect more drastically to A than B series. Therefore, surface area ranges between 35 and 121 m^2/g for A series whereas it is in the range 52–83 m^2/g for B one. In the case of A series, the highest surface area corresponded to TiO_2A-US whereas TiO_2B-R exhibited the highest value within B series. If all systems are considered, the highest surface area was obtained through the use of TTIP as the titanium precursor and sonication as the ageing method (TiO_2A-US).

Raman spectra of all systems exhibited three main peaks centered at ca. 399, 518 and 640 cm^{-1}, attributed to fundamental vibrational modes of anatase B_{1g}, $A_{1g} + B_{1g}$ and E_g, respectively [19]. Such peaks were already present in precursor gels for TiO_2B-R and TiO_2B-MW, though their full-width at half-maximum (FWHM) values were greater than those of the corresponding calcined systems. Therefore, as far as B series is concerned, ageing under reflux or microwave treatment induced the crystallization of TiO_2 in its anatase form which accounts for the absence of the glow exotherm in the DTA profiles of precursor gels of TiO_2B-MW and TiO_2B-R. For such systems, calcinations at 500 °C only resulted in an increase in the crystallite size.

X-Ray diffraction patterns of all systems confirm the results obtained by Raman spectroscopy as concerns the predominance of TiO_2 in its anatase form in all cases. Nevertheless, as shown in Table 1, a certain amount of brucite or rutile is present in some cases. If all systems are considered, sonication is the only ageing method which ensured obtaining 100% anatase, irrespective of the titanium precursor used.

In order to obtain some information on the potential application in photocatalysis of our solids UV spectra were obtained. UV–vis data collected in Table 1 seems to indicate that the use of titanium tetrachloride as the Ti precursor leads to lower band gap values than titanium tetraisopropoxide. As regards A series, the ageing method had no effect on the absorption threshold whereas as far as B series is concerned all systems but TiO_2B-MW exhibited similar band gap values.

3.1.2. Photocatalytic experiments

Results found for all pure-titania systems in photocatalytic selective oxidation of propan-2-ol after a time-on-stream of 5 h, in terms of molar conversion and selectivity to acetone and CO_2 are depicted in Fig. 2. For the sake of comparison, catalytic performance of Degussa P25 has also been included. As can be seen, higher conversions are obtained for A series than for B one. If the ageing method is considered, the change from the conventional magnetic stirring method to either microwave, reflux or ultrasonic treatment results in an increase in conversion whereas selectivity to acetone hardly changes (ca. 75% in all cases). Finally, apart from CO_2 (ca. 4–6%) some other products detected include acetaldehyde, propene or acetic acid whose mechanism of obtaining is discussed elsewhere [20].

3.2. Pt-doped titania system

The fact that as reported above A series led to better results in terms of conversion than B one and that ultrasonic treatment ensured obtaining 100% anatase affording a catalyst with quite a high surface area (121 m^2/g) when TTIP was used as the titanium precursor, prompted us to choose such conditions for incorporation of Pt by the precipitation method, thus obtaining the system labelled as Pt-AS.

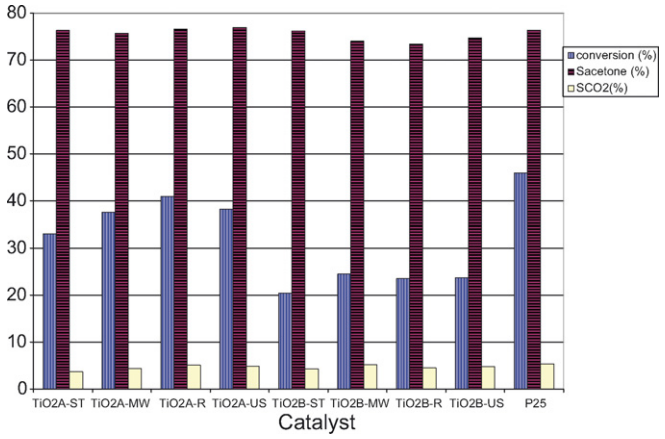

Fig. 2. Results obtained for gas-phase selective photooxidation of 2-propanol with all the pure-titania systems described in the present study in terms of molar conversion (%), selectivity to acetone (%) and selectivity to CO_2 (%) after a time-on-stream of 5 h. For the sake of comparison, results obtained with Degussa P25 have also been included.

3.2.1. Characterization of platinum-containing titania systems

TG-DTA profiles of precursor gels of TiO_2A-US and Pt-AS (not shown) are quite similar with an endothermal peak at ca. 115 °C attributed to loss of water and an exothermal peak at 421 or 436 °C for TiO_2A-US gel and Pt-AS gel, respectively, associated to crystallisation to anatase. Therefore, the presence of platinum only induces a slight retard in crystallisation of titania. It is also noteworthy that there is no weight loss above calcination temperature (500 °C).

Once Pt-AS system had been synthesized, Pt/Ti at.% was determined by ICP-MS. Obtained value (0.5%) is half the nominal value. The fact that at pH value used for the precipitation (pH 9) some soluble species of platinum (e.g., $PtOH^+$ and $Pt(OH)_2(aq)$) may exist could account for that [21].

TPR profile of Pt-AS system is shown in Fig. 3. The one obtained for the corresponding pure-titania system (TiO_2A-US) has also been included for comparative purposes. Pt-AS exhibit three main reduction peaks centered at ca. 60 (with a shoulder at 128 °C), 395 and 616 °C. There are some discrepancies in the literature concerning both the appearance of reduction peaks of

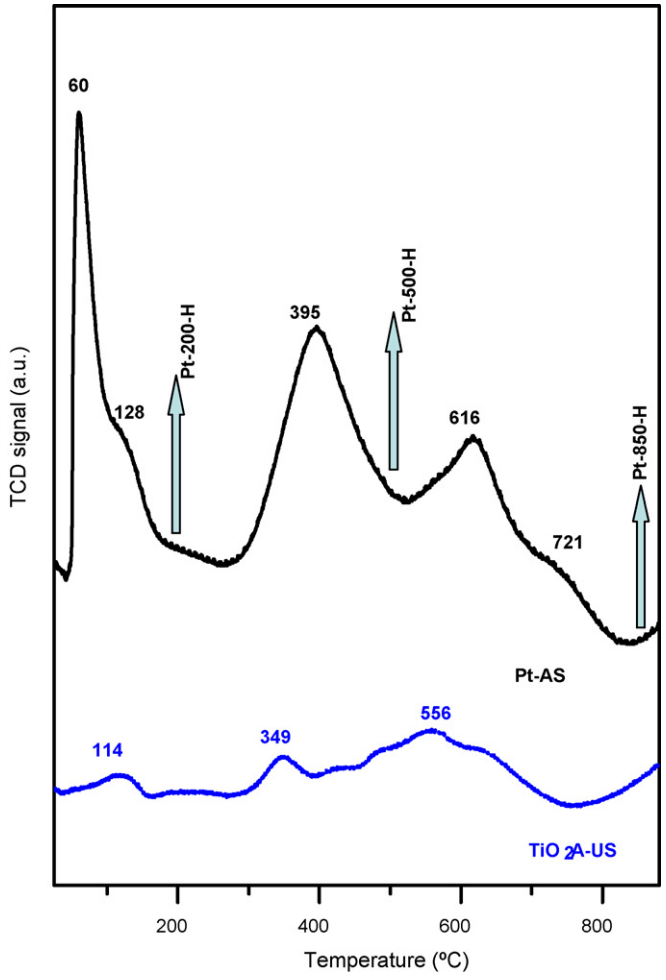

Fig. 3. TPR profiles of Pt-AS and the corresponding pure-titania system. The vertical arrows indicate the temperatures selected for reductive treatment of Pt-AS system, thus yielding the catalysts labeled as Pt-200-H, Pt-500-H and Pt-850-H.

Pt-containing systems and their interpretation, probably as a result of the different nature of the solids described (e.g., use of diverse supports). However, peaks observed at low temperatures are generally attributed to reduction of PtO_x species whereas those appearing at high temperatures are associated to the reduction of TiO_2 catalyzed by Pt through the so-called strong metal-support interaction (SMSI). In this sense, the peak centered at 60 °C could be associated to the reduction of PtO_x whereas those peaks centered at ca. 395 and 616 °C could be attributed to the hydrogen uptake resulting from the interaction of Pt and TiO_2. In a TPR study of a Pt/Al_2O_3 system, Hwang and Yeh [22] distinguished a peak at −25 °C assigned to reduction of surface PtO (which could account for our system getting darker on H_2 flow at 0 °C), and two additional ones at 50 and 100 °C attributed to the reduction of PtO and PtO_2, respectively. These two latter peaks could correspond to the one we observed at 60 °C and the shoulder at 128 °C. In separate studies on Pt/TiO_2 systems da Silva et al. [23] and Panagiotopoulou et al. [24] found two reduction peaks. A first one centered at ca. 175–190 °C was assigned to the reduction of PtO whereas the second one, appearing at 400–500 °C was attributed to the reduction of TiO_2 catalyzed by Pt through strong metal-support interaction (SMSI). In our case, SMSI effect could account for the appearance of either one or the two high temperature reduction peaks (centered at 395 and 616 °C in Pt-AS system).

In order to gather additional information on the above-mentioned effects and to study the influence of initial oxidation state of platinum on its photocatalytic performance in propan-2-ol photocatalytic selective oxidation, two intermediate reduction temperatures (200 and 500 °C) corresponding to two valleys between peaks in TPR profile together with the final temperature (850 °C) were selected for thermal treatment of Pt-AS system (see Fig. 3). For comparative purposes, oxidations at the same final temperature (850 °C) were performed both in synthetic air flow (Pt-850-AIR) and in static air (Pt-850-F).

Some other features corresponding to characterization of Pt-containing systems are summarized in Table 2. As regards reductive treatment, heating at 200 °C (Pt-200-H) did not change textural and structural properties of Pt-AS. Therefore, specific surface area remains 57 m^2/g, crystallite size 21 nm and the catalyst consist in 100% anatase. Reduction at 500 °C (Pt-500-H) results in a slightly decrease in surface area of Pt-AS (from 57 to 50 m^2/g) whereas crystallite size slightly increases (from 21 to 23 nm). This small change is explained by the fact that Pt-AS was obtained by calcination of the precursor gel at 500 °C, although in static air. On the other hand, reduction (Pt-850-H) or oxidation treatment (Pt-850-F and Pt-850-AIR) at a temperature significantly higher than the one at which Pt-AS was synthesized (500 °C) resulted in a dramatic decrease in surface area, accompanied by a significant increase in the TiO_2 crystallite size and its transformation from 100% anatase to 100% rutile. Reductive treatment results in greater TiO_2 crystallites (77 nm) than oxidative one (53 and 66 nm for calcination in static air or air flow, respectively).

XRD diffractograms corresponding to all Pt-containing systems are depicted in Fig. 4. Platinum metal and platinum

Table 2
Summary of the most remarkable features concerning characterization of Pt-containing titania systems

Photocatalyst	XRD		N_2 isotherms	ICP-MS	XPS				
	Crystal phases[a] (%)	Crystallite size (nm)	S_{BET} (m^2/g)	Pt/Ti (at.%)	Ti($2p_{3/2}$) Binding energy (eV)	O(1s) Binding energy (eV)	Pt/Ti (at.%)	C (at.%)	O/Ti
Pt-AS	100%A	21	57		458.4	529.6	–[b]	2.98	1.86
Pt-200-H	100%A	21	57				Not determined		
Pt-500-H	100%A	23	50						
Pt-850-H	100%R	77	6		458.2	529.5	3.50	3.75	1.92
Pt-850-AIR	100%R + Pt^0	66	6	0.5	458.4	529.8	0.88	3.84	1.92
Pt-850-F	100%R + Pt^0	53	8		458.2	529.4	1.06	4.47	1.98
Pt-850-AIR after reaction		Not determined			458.3	529.7	0.98	5.73	1.97
Pt-850-H after reaction					458.3	529.6	3.74	4.63	2.06

[a] A and R denote anatase and rutile, respectively.
[b] Quantification of platinum at.% present at the surface of Pt-AS was not possible since the intensity of Pt(4f) peak was very small.

oxide phases could be identified in the XRD patterns through its reflections at $2\theta = 39.73$, 46.24, and 67.41 (Pt metal, JCPDS 4–802) and $2\theta = 34.8$, 42.5, and 54.9 (PtO, JCPDS 42–866). Interestingly, the presence of Pt^0 was detected in the systems resulting from oxidation at 850 °C (Pt-850-F and Pt-850-AIR) but not in the Pt-AS (calcined at 500 °C) nor in the ones obtained after reduction at any temperature (Pt-200-H, Pt-500-H or Pt-850-H). The formation of Pt^0 on oxidation at high temperatures, has already been reported in the literature. Thus, Hwang and Yeh [22] described the decomposition of PtO_2 already at $T \approx 600$ °C according to the following sequence of platinum oxidation:

$$Pt \rightarrow PtO \rightarrow PtO_2 \rightarrow Pt$$

The particles of Pt^0 in Pt-850-F and Pt-850-AIR could be greater than the ones of the other systems (Pt-AS, Pt-200-H, Pt-500-H and Pt-850-H) which together with the low Pt-content (0.5%) could account for the absence of a peak of Pt^0 or any other Pt-species in the XRD of the latter systems. Nevertheless, the platinum oxidation state and the Pt crystal size of the systems should be later checked by XPS and TEM.

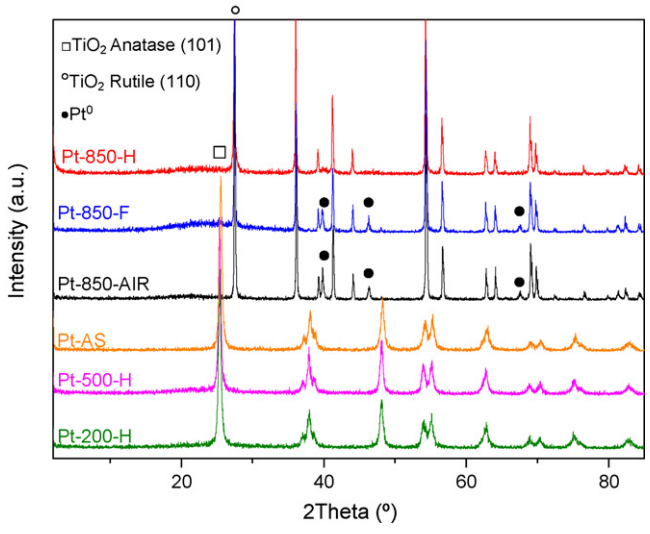

Fig. 4. X-ray diffraction patterns corresponding to the Pt-contaning titania.

3.2.2. *Photocatalytic performance of platinum-containing systems*

The catalysts above described were tested in the gas-phase photocatalytic selective oxidation of propan-2-ol. Results obtained for all Pt-systems are shown in Fig. 5. As can be observed, irrespective of the treatment (oxidative or reductive), the calcination of Pt-AS resulted in an improvement in photocatalytic activity. This is especially significant in the case of Pt-850-AIR and Pt-850-F. So much so, that both systems yielded better conversions than Degussa P25, the most-widely used photocatalyst. This is particularly remarkable considering that those systems consist in very low surface area rutile titania particles. Therefore, such systems should have exhibited worse catalytic performance than Pt-AS since, as pointed out by Enríquez et al. [25] as the sintering temperature increases the

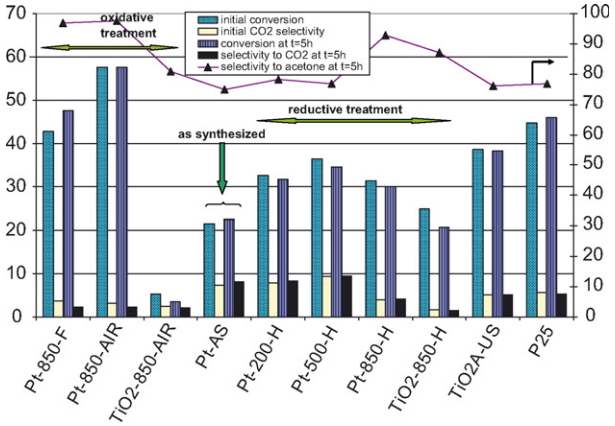

Fig. 5. Results obtained for gas-phase selective photooxidation of 2-propanol with all the Pt-containing titania systems in terms of molar conversion (%) and selectivity to CO_2 (%) – both initially and for a time-on-stream of 5 h – and final selectivity to acetone ($t = 5$ h). For the sake of comparison, results obtained with TiO_2A-US and such a system calcined at 850 °C either in synthetic air (TiO_2-850-AIR) or hydrogen (TiO_2-850-H) flow as well as catalytic behaviour of Degussa P25 have been included.

reduced recombination rate should be probably outweighed by the reduced surface area. In other words, the improvement we observe should be associated to the presence of platinum and the proposed SMSI interaction between Pt and TiO_2, as confirmed by the fact that the corresponding pure-titania systems (TiO_2-850-AIR and TiO_2-850-H) exhibited lower conversions than TiO_2A-US.

In order to rule out the possibility of thermal activity, an experiment on Pt-AS with a heat ray cutting filter (Hamamatsu Ref. A7028-03, cut wave length 400–700 nm) was performed. Under such conditions, UV transmittance dropped from 1.1 to 0.9 W cm^{-2}. Consequently, conversion after 5 h on-stream dropped from 19.7 to 16.3 (17% decrease). Another experiment in which light intensity was adjusted to 83% of the total (without filtering) was carried out and conversion obtained after 5 h on-stream was 16.4%. Therefore, no significant thermal effect is observed under our experimental conditions and, consequently, photocatalytic activity is to account for propan-2-ol transformation.

Finally, a look at results shown in Fig. 5 allows us to conclude that selectivity to acetone is higher with rutile than with anatase particles. Therefore, its value increases from ca. 75% for all pure-anatase systems (P25, TiO_2A-US, Pt-AS, Pt-200-H or Pt-500-H) up to 81 or 85% for TiO_2-850-AIR and TiO_2-850-H, respectively. An additional increase in selectivity to acetone is obtained for Pt-AS calcined at 850 °C, with a maximum value of 97.7% for Pt-850-AIR system.

3.2.3. TEM and XPS analyses on Pt-doped systems

In order to get some information on the reasons for the improvement of photocatalytic performance of TiO_2 systems on the introduction of platinum and calcinations at high temperature, TEM and XPS analyses were carried out.

TEM micrographs of Pt-850-AIR and Pt-850-H are compared in Fig. 6. In the former case, agglomerates of platinum particles with a diameter of ca. 50 nm are observed whereas smaller and more uniformly distributed platinum particles are distinguished in the latter case. The greater size of platinum particles in Pt-850-AIR could explain the detection of peaks of Pt^0 in the corresponding XRD. Finally, EDX study of the systems suggests a greater surfacial Pt-content in Pt-850-H than in Pt-850-AIR.

The determination of the nature and oxidation state of Pt species (Pt^0, Pt^{2+} and Pt^{4+}) is normally accomplished using XPS technique and in particular by means of the Pt(4f) peak study. It is known that metallic Pt^0 has binding energies of 70.7–70.9 and 74.0–74.1 eV for $4f_{7/2}$ and $4f_{5/2}$ electrons, respectively [26,27]. In oxidized states, Pt^{2+} and Pt^{4+} exhibit much higher

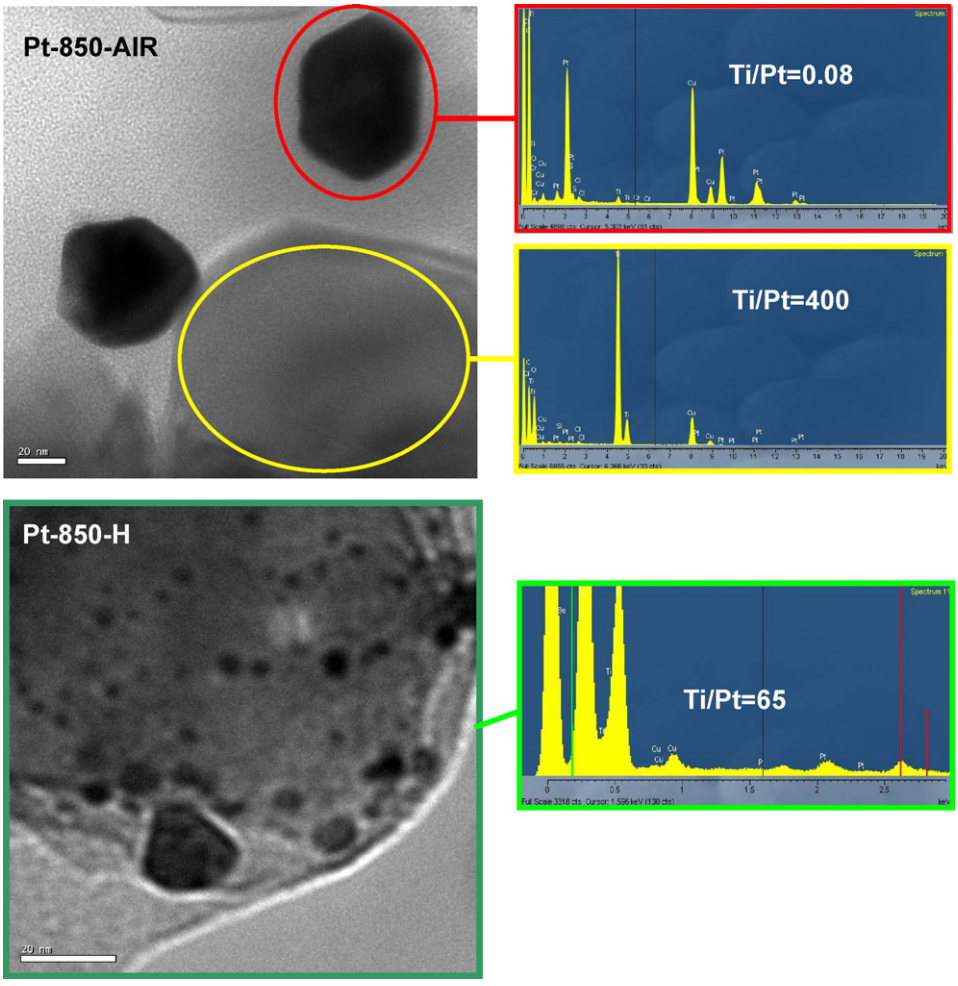

Fig. 6. TEM micrographs and EDX analyses of Pt-850-AIR and Pt-850-H systems.

binding energies: 72.8–73.1 eV ($4f_{7/2}$) and 76.3–76.4 eV ($4f_{5/2}$) for Pt^{2+} and 74.6–74.9 eV ($4f_{7/2}$) and 78.1–78.2 eV ($4f_{5/2}$) for Pt^{4+} [27–30].

The effect of several treatments (calcination, reduction, oxidation, etc.) on the oxidation state of Pt/TiO_2 has been investigated by XPS. Fig. 7A shows the XPS results of the Pt/TiO_2 samples after the indicated treatment. In the region of platinum, the original sample (Pt-AS), showed a XPS profile which is relatively complex in which peaks at 72.4, 75.1 eV in addition to a shoulder at 78.0 eV can be identified. Thus, it can be inferred that in the original sample the valence state of Pt is Pt^{2+}/Pt^{4+}. After reduction in H_2/Ar flux at 850 °C (Pt-850-H), two main peaks at 70.4 and 73.8 eV are observed thus indicating the presence of Pt^0. However, the values are slightly shifted to lower binding energies as compared to data reported in the literature [26,27] (around 0.3 eV) which can be indicative of SMSI effect as reported for Pt/CeO_2 [31] and Pt/TiO_2 [32] catalysts. Therefore, electrons could be donated from TiO_2 to Pt, thus forming $(Pt)_n^{\sigma-}$ species.

The oxidation treatment of the original sample, either in air flux or calcination in air at 850 °C (Pt-850-AIR and Pt-850-F), led to a Pt-XPS profile in which peaks around 70.1 and 73.4 eV are identified together which a shoulder around 75.0 eV indicating the presence of a mixture of Pt^0 (predominant) and Pt^{2+} at the catalyst surface. This is consistent with XRD results with indicated the presence of Pt^0. The shift in the position of Pt^0 signals for Pt-850-AIR and Pt-850-F (ca. 0.6 eV), is even more pronounced than for Pt-850-H indicating negatively charged platinum particles, thus suggesting the electron transfer from TiO_2 to Pt through a strong metal-support interaction. Under UV irradiation, SMSI effect could avoid electron–hole recombination thus accounting for the improvement in catalytic activity of samples calcined at 850 °C as compared to Pt-AS. Moreover, the more pronounced such an effect (case of Pt-850-AIR and Pt-850-F), the better the catalytic performance.

A comparison of XPS results for Pt-850-AIR before and after reaction, allow us to conclude that the oxidation states of Pt (mixture of Pt^0/Pt^{2+}) are not altered after the photocatalytic oxidation of 2-propanol although the shoulder at 75.0 seems to be more pronounced. A similar conclusion can be drawn if XPS of Pt-850-H before and after the reaction are compared. Thus, the oxidation states of Pt in Pt-850-H (mainly as Pt^0) are not altered by the photocatalytic oxidation of 2-propanol.

XPS data concerning TiO_2 matrix for Pt/TiO_2 samples are shown in Table 2. The quantification of the platinum at.% present at the surface of Pt-AS, was not carried out because the very small intensity of the Pt(4f) peak observed near to the Ti(3s) peak. Therefore, we can assume for this sample that the amount of surface Pt is very low (even lower than those estimated for Pt-850-AIR, Pt-850-F or Pt-850-AIR after reaction) indicating that, for Pt-AS, a great deal of platinum species are located into the TiO_2 particles. Treatment at 850 °C leads in all cases to an increase in surfacial Pt-content as compared to Pt-AS, which is especially remarkable in the case of Pt-850-H. Therefore, in that sample Pt-content (3.5 Pt/Ti at.%) is seven times the bulk content as determined by ICP. The lower Pt surfacial content of samples treated under oxygen as compared to the one obtained on hydrogen flow could indicate that in Pt-850-AIR, and Pt-850-F samples Pt^0 particles are

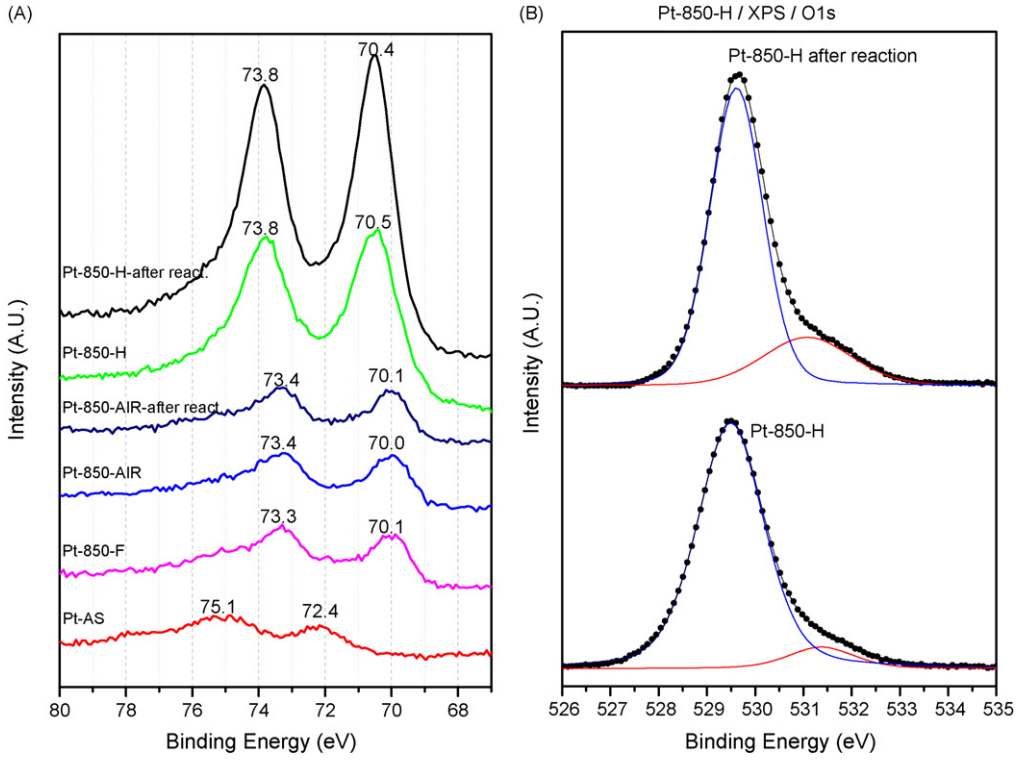

Fig. 7. Pt(4f) XP spectra of the different systems (A) and deconvolved O(1s) XP spectra of Pt-850-H system before and after the gas phase photocatalytic selective oxidation of propan-2-ol (B).

probably decorated by a partial TiO_2 film, whereas the Pt^{2+} seems to be forming a pre-surface layer.

Binding energies for Ti($2p_{3/2}$) peaks at 458.3 ± 0.1 eV clearly correspond to Ti^{4+} in TiO_2 structure. The analyses of the Ti(2p) spectra did not allow detecting any considerable amount of Ti^{3+} ions in the samples, which would be expected from SMSI effect. However, by examining the chemical composition on the surface from XPS, it is worth mentioning that the O/Ti ratios for all samples are very close to the stoichiometric value (O/Ti $\sim$ 2.0) although, except for Pt-AS, the O/Ti ratios are slightly below the stoichiometric value. These results allow us to expect (except for Pt-850-H after reaction) a certain number of oxygen vacancies in the systems.

Regarding O(1s) band, it is noteworthy that for all samples a main peak is detected at a binding energy of 529.6 ± 0.2 eV together with a weak peak centred at 531.6 ± 0.2 eV. The main peak at around 529.6 eV could be ascribed to lattice oxygen in TiO_2, while the signal at ca. 531.6 eV could be associated to oxygen probably as carbonate species as well as surface hydroxyl groups which seem to be present in all samples. In Fig. 7B O(1s) spectra corresponding to Pt-850-H before and after reaction are depicted. As can be observed, there is an increase in the intensity of peak at ca. 531.5 eV after 5-h on-stream in propan-2-ol photocatalytic oxidation which could be attributed to the formation of carbonates on the surface. Therefore, C at.% increases from 3.75 to 4.63% (see Table 2). Such carbonate species would contribute to increase surfacial oxygen content which could explain the increase in O/Ti ratio with time-on-stream (Table 2, last column). Moreover, since Pt surfacial content (not represented in Table 2) does not change with time-on-stream but atomic Ti% slightly decreases, carbonate species seems to form predominantly on Ti particles, which could explain the slight increase in Pt/Ti at.% with time on stream (see Table 2). The generally accepted mechanism for oxidations on Pt-doped titania by which propan-2-ol would adsorb on titania whereas oxygen would do on Pt particles could account for the preferential formation of carbonate species on titania.

4. Conclusions

The above-mentioned results allow us to draw the following conclusions:

(1) Different titania systems were synthesized by the sol–gel process starting from two different titanium precursors (titanium tetraisopropoxide and titanium choride) and varying the ageing method: magnetic stirring, reflux, ultrasonic and microwave radiation.
(2) All the systems were tested for the gas-phase selective photoxidation of propan-2-ol. Optimisation of the synthetic conditions led to the choice of titanium tetraisopropoxide as the titanium precursor and sonication as the method for ageing of the gel. Therefore, a system with a large surface area and consisting of 100% anatase was achieved. The optimized synthetic procedure was applied to obtain a Pt-doped titania system by coprecipitation.
(3) The effect of the oxidation/reduction treatment of the Pt-doped system on its catalytic performance was studied. Interestingly, both oxidation and reduction at 850 °C resulted in an increase in molar conversion and selectivity to acetone. Such improvement in catalytic behaviour was especially remarkable in the case of oxidative treatment which led to better results than for Degussa P25.
(4) XPS analyses showed that systems treated at 850 °C consisted of negatively charged platinum particles, thus suggesting the electron transfer from TiO_2 to Pt (strong metal support interaction, SMSI). Moreover, the greater the SMSI effect, the better the catalytic performance. Such SMSI effect would prevent electron–hole recombination which could explain that, even though oxidation/reduction treatment at 850 °C had led to a decrease in surface area and transformation of anatase to rutile, an improvement in photocatalytic activity was observed.

Acknowledgements

The authors wish to acknowledge financial support from the Consejería de Educación y Ciencia of the Junta de Andalucía (Project FQM 191) and the Spanish Ministerio de Educación y Ciencia (Projects CTQ 2005-04080/BQU and CTQ 2004-05734-C02-02, co-financed with FEDER funds). CA Concorde Project NMP2-CT-2004-505834 is also gratefully acknowledged. Finally, Dr. Colmenares is thankful to the Spanish Ministerio de Educación, Cultura y Deportes for a post-doctoral fellowship and A. Marinas to Junta de Andalucía for a contract.

References

[1] K.I. Shimizu, H. Akahane, T. Kodama, Y. Kitayama, Appl. Catal. A 269 (2004) 75.
[2] C.E. Taylor, Catal. Today 84 (2003) 9.
[3] X. Zhang, F. Zhang, K.-Y. Chan, Mater. Chem. Phys. 97 (2006) 384.
[4] P. Pichat, New. J. Chem. 11 (1987) 135.
[5] S.J. Tauster, S.C. Fung, R.L. Garten, J. Am. Chem. Soc. 100 (1978) 170.
[6] M. Bowker, P. Stone, R. Bennett, N. Perkins, Surf. Sci. 497 (2002) 155.
[7] M. Zhang, Z. Jin, Z. Zhang, H. Dang, Appl. Surf. Sci. 250 (2005) 29.
[8] M. Bowker, P. Stone, P. Morrall, R. Smith, R. Bennett, N. Perkins, R. Kvon, C. Pang, E. Fourre, M. Hall, J. Catal. 234 (2005) 172.
[9] D.R. Jennison, O. Dulub, W. Hebenstreit, U. Diebold, Surf. Sci. 492 (2001) L677.
[10] F. Pesty, H.P. Steinruck, T.E. Madey, Surf. Sci. 339 (1995) 83.
[11] J.C. Colmenares, M.A. Aramendia, A. Marinas, J.M. Marinas, F.J. Urbano, Appl. Catal. A 306 (2006) 120.
[12] S.A. Larson, J.A. Widegren, J.L. Falconer, J. Catal. 157 (1995) 611.
[13] S. Sakthivel, H. Kisch, Angew. Chem. Int. Ed. 42 (2003) 4908.
[14] J.E. Herrera, D.E. Resasco, J. Phys. Chem. B 107 (2003) 3738.
[15] Y. Miyake, H. Tada, J. Chem. Eng. Jpn. 37 (2004) 630.
[16] H. Xie, Q. Zhang, T. Xi, J. Wang, Y. Liu, Thermochim. Acta 381 (2002) 45.
[17] S. Brunauer, P.H. Emmett, E.J. Teller, J. Am. Chem. Soc. 60 (1938) 309.
[18] J.H. De Boer, The Structure and Properties of Porous Materials, Butterworths, London, 1958.
[19] W.X. Zhang, C.B. Wang, H.L. Lien, Catal. Today 40 (1998) 387.
[20] M.A. Aramendía, J.C. Colmenares, S. López-Fernández, A. Marinas, J.M. Marinas, F.J. Urbano, Catal. Today, in press.
[21] M. Azaroual, B. Romand, P. Freyssinet, J.R. Disnar, Geochim. Cosmochim. Acta 65 (2001) 4453.
[22] C.P. Hwang, C.T. Yeh, J. Mol. Catal. A 112 (1996) 295.

[23] A.B. da Silva, E. Jordao, M.J. Mendes, P. Fouilloux, Appl. Catal. A 148 (1997) 253.
[24] P. Panagiotopoulou, A. Christodoulakis, D.I. Kondarides, S. Boghosian, J. Catal. 240 (2006) 114.
[25] R. Enríquez, A.G. Agrios, P. Pichat, Catal. Today 120 (2007) 196.
[26] T. Teranishi, M. Hosoe, T. Tanaka, M. Miyake, J. Phys. Chem. B 103 (1999) 3818.
[27] Y. Nagai, H. Shinjoh, K. Yokota, Appl. Catal. B 39 (2002) 149.
[28] T. Wang, A. Vazquez, A. Kato, L.D. Schmidt, J. Catal. 78 (1982) 306.
[29] V. Romanovskaya, M. Ivanovskaya, P. Bogdanov, Sens. Actuators B 56 (1999) 31.
[30] S. Zafeiratos, G. Papakonstantinou, M.M. Jacksic, S.G. Neophytides, J. Catal. 232 (2005) 127.
[31] M. Abid, V. Paul-Boncour, R. Touroude, Appl. Catal. A 297 (2006) 48.
[32] H. Iida, A. Igarashi, Appl. Catal. A 303 (2006) 192.